16

Fast and Accurate Tactile Sensor System for a Human-Interactive Robot

Toshiharu Mukai, Shinya Hirano and Yo Kato
Bio-Mimetic Control Research Center, RIKEN
Japan

1. Introduction

With the advent of the aging society, the demand for nursing care for the elderly is becoming much larger. The application of robotics to helping on-site caregivers is consequently one of the most important new areas of robotics research. Such human-interactive robots, which share humans' environments and interact with them, should be covered with soft areal tactile sensors for safety, communication, and dextrous manipulation.

Tactile sensors have interested many researchers and various types of tactile sensors have been proposed so far. Many tactile sensors have been developed on the basis of micro-electro-mechanical system (MEMS) technology (for example, (Suzuki, 1993; Souza & Wise, 1997)). They have a high-density and narrow covering area realized by applying MEMS technology, and as a result, are not suitable for covering a large area of a robot's surface. Some tactile sensors suitable for use on robot fingers or grippers have also been developed (Nakamura & Shinoda, 2001; Yamada et al., 2002; Shimojo et al., 2004). Many of them have the ability to detect tangential stress and can be used in grasping force control. Their main target is robot fingers, and consequently they were not designed to cover a large area. There are also commercially available tactile sensors such as those offered by Tekscan (Tekscan, 2008) based on pressure-sensitive ink or rubber, and KINOTEX™ tactile sensors (Reimer & Danisch, 1999) utilizing the change in the intensity of light scattered by the covering urethane foam when deformed. However, they are not sufficiently accurate because of strong hysteresis and creep characteristics.

The idea of covering a large area of a robot's surface with soft tactile skinlike sensors is attracting researchers (Lumelsky et al., 2001). Some human-interactive robots for which a large area of their surface is covered with soft tactile sensors have actually been developed (Inaba et al. 1996; Tajima et al. 2002; Kanda et al. 2002; Mitsunaga et al. 2006; Ohmura et al., 2006; Ohmura & Kuniyoshi, 2007). However, the tactile sensors are not suitable for human-interactive robots, particularly when physical labor using tactile sensation is required. For example, one tactile sensor in (Tajima et al. 2002) has only 3 values as its output, and another tactile sensor in (Tajima et al. 2002) is gel-type and cannot be used over a long period because of the evaporation of the contained water. The tactile sensor in (Mitsunaga et al. 2006) has only 56 elements in total. Flexible fabric-based tactile sensors using an electrically conductive fabric have also been proposed for covering a robot (Inaba et al. 1996), but the

Source: Sensors, Focus on Tactile, Force and Stress Sensors, Book edited by: Jose Gerardo Rocha and Senentxu Lanceros-Mendez,
ISBN 978-953-7619-31-2, pp. 444, December 2008, I-Tech, Vienna, Austria

sensors are binary switches, and are difficult to fabricate. To our knowledge, the tactile sensor used by (Ohmura et al., 2006) has been the most successful for covering a large area of a robot's surface. This tactile sensor is based on similar technology to KINOTEX™, but uses tiny photoreflectors under urethane foam instead of the combination of light-emitting diodes, photodetectors, and fiber-optic cables. The tactile sensor is fabricated on a flexible substrate using photoreflectors and circuitry for driving and communication. Their sensor is suitable for detecting tactile contact, but the principle of their sensor depends on the deformation of urethane foam, which inevitably causes strong hysteresis and creep characteristics. Hence, when accuracy is needed, for example, when tactile feedback control is required, we need more accurate tactile sensors.
For the realization of a robot with tactile sensation, a real-time acquisition and integration system for gathering tactile sensor data distributed all over the robot's body is also needed. When a robot is covered with tactile sensors, the problems of huge computational load and a large number of cables arise. Localized processing is an effective solution, and tactile sensors with distributed processors have been developed. For example, the robot in (Tajima et al. 2002) had multiple MPUs connected by a serial bus, and that in (Ohmura et al., 2006) used a network composed of local serial buses and a custom-designed ring-type network.
We are developing a robot named RI-MAN (Odashima et al., 2006; Odashima et al., 2007; Mukai et al., 2008), shown in Fig. 1, with soft areal tactile sensors, as a platform for physical human-robot interaction research. Our ultimate goal for RI-MAN is to help nurse elderly people in their daily lives, and this inevitably involves performing hard physical tasks in complex environments such as hospitals and homes. RI-MAN can physically interact with humans via soft and whole-body interaction. Having a similar size to a human (158 cm in height and 100 kg in weight) and a smooth surface without bumps, RI-MAN can perform the task of lifting up a dummy human in its arms. To skillfully perform such tasks that involve physical contact with humans, RI-MAN is equipped with soft areal tactile sensors in five places, the chest and the right and left of the upper arms and forearms.

Fig. 1. RI-MAN with tactile sensors for physical human-robot interaction research

We have developed soft areal tactile sensors for RI-MAN by embedding semiconductor pressure sensors as pressure-sensing elements in an elastic body (Mukai, 2004; Mukai, 2005), as well as their controllers that can realize localized processing and integration through the network in a robot. Our primary target is the achievement of physical tasks using tactile sensation, such as lifting up a human. Because semiconductor pressure sensors have little hysteresis or creep, our sensors also have an accurate response, although the elastic body covering causes a little hysteresis and creep. The sensor should be able to detect wide range of pressure from light finger touch to the load of a human held by the robot arms. The sampling speed and accuracy should be enough for usage in sensor feedback control. Our tactile sensors satisfy the requirements for human-interactive robots.

In this paper, we report our tactile sensor, as well as its implementation in a robot. After this introduction, we first describe specifications necessary for tactile sensors in human-interactive robots. Next we describe the structure and fabrication method of our tactile sensor. Next we describe the implementation of the tactile sensor system in our robot RI-MAN. Then we report experimental results of the sensor itself and sensor usage in the robot. Finally we conclude our paper.

2. Specifications

In this research, we are aiming to develop soft areal tactile sensors that cover the surface of a human-interactive robot, and provide a pressure strength and distribution that can be used to control the manipulation of objects. To make this possible, we need sensors that are soft like human skin and can cover a large area of a robot's curved surfaces, for safety and affinity. We are developing such sensors by embedding small semiconductor pressure sensors as pressure-sensing elements in an elastic body. The elastic body also contributes to the removal of undesirable insensitive regions by giving interpolation ability to the sensor. The preciseness of semiconductor pressure sensors can yield high-accuracy tactile sensors. Considering the application of tactile sensors to human-interactive robots, we determined the necessary specifications of our tactile sensor system as follows. First, we require a spatial resolution of about 10 to 20 mm, referring to the approximately 10 mm resolution of the human palm and 40 mm of the human forearm. Except for the fingertips, this resolution is sufficient to realize a resolution similar to that of a human. Next, we consider the measurable pressure range. When a robot holds a person of 60 kg in its arms with a contact area of 20×20 cm^2, the average pressure is 14.7 kPa. Using a safety factor of 6, we require a pressure range of 0 to 88 kPa. Next, we discuss the measurement resolution. Considering feedback control using tactile sensation, we require a measurement resolution in which the contact force caused by typical human-robot interaction is expressed by more than 5 bits. We believe that feedback control is smooth if the value is expressed with this resolution.

Tactile sensors for robots require tactile sensor controllers suitable to be used in robots. It is desirable that each controller be in the vicinity of the tactile sensor, with short connections between sensors and controllers, because the connection requires a large number of cables. This also reduces electric noise because tactile sensor output is analog, while we can use digital signals for connections among controllers. This requires the following. Controllers must be able to form a network for sensor data integration in the robot. Controllers must be sufficiently small to fit in a robot. Controllers must calculate abstract compressed features from sensor data. Such compressed features are carried through a narrower bandwidth, to simplify connection in robot and reduce the possibility of cable breakdown. We also require that the sampling speed be sufficiently fast for our robotic purposes. The sampling speed depends on the performance of both the sensor and its controller, so that the total system should be designed to satisfy this requirement. The sampling speed of sensor data and the communication speed among controllers should agree with the robot control period. It is empirically known that, for stable and smooth feedback control, the sampling frequency should be more than 10 times the resonance frequency of the controlled object (Paul, 1981). In general, robots have a resonance frequency of 1 to 50 Hz, so that the required sampling frequency is 10 to 500 Hz, which corresponds to a sampling period of 2 to 100 ms (RSJ, 2005).

3. Structure and fabrication method of the tactile sensor

3.1 Basic structure and components

As pressure-sensing elements, we adopted FUJIKURA FPBS-04A pressure sensors (Fig. 2). These are very small (φ5.8 mm) piezoresistive semiconductor pressure sensors that can detect absolute pressure between 42.6 and 434.7 kPa. Each sensor has a resistive bridge on its diaphragm and the output changes almost linearly with the applied pressure.

Fig. 2. Small FUJIKURA semiconductor pressure sensors

To reduce the number of cables leading out from the tactile sensors, we designed a scanning circuit, an example of which including 4x4 elements is shown in Fig. 3. By changing switches, we can select a row and a column to obtain the output from the selected element. In this example, the top-left element is selected by switching. All outputs of the pressure-sensing elements are obtained by scanning this array. The actual circuit we made has an array of 8x8 pressure-sensing elements with an 18 mm pitch. This pitch was determined to satisfy the above requirement to realize a spatial resolution similar to a human. We fabricated the circuit as a flexible printed circuit (FPC), so that it can be fit onto a 2D-curved surface (which can be expanded into a 2D plane) because of its flexibility. We call the FPC sheet with the pressure-sensing elements and other electronic parts as 'sensor sheet'. To mount it onto a free-curved surface (which cannot be expanded into a 2D plane), we designed the circuit so that all the wiring is concentrated into a comb-shaped region. Thus, the sensor sheet can be cut into a shape consisting of thin regions. After cutting, the sheet can be wound onto a free-curved surface, as shown in Fig. 4, if the curvature is not too sharp. In addition, we designed the circuit all of which wiring concentrates into a comb-shaped region, so that it works if the central part remains even when the marginal parts are cut off. Therefore it can be applied to a smaller surface than the original sensor sheet. To reduce cables, we also put analog switches and an instrumentation amplifier on the FPC. As a result, the number of cables has become 10. As the instrumentation amplifier, we adopted a digital amplifier that can select its gain from 1, 2, 4, and 8. If this amplifier gain needs to be controlled, additional two cables are needed.

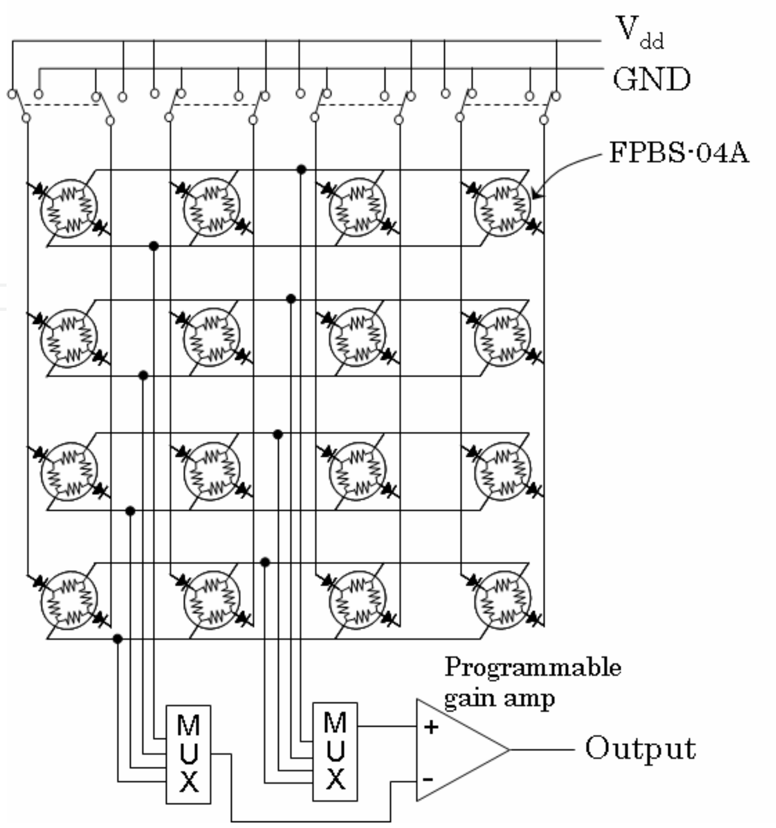

Fig. 3. Circuit of our tactile sensor

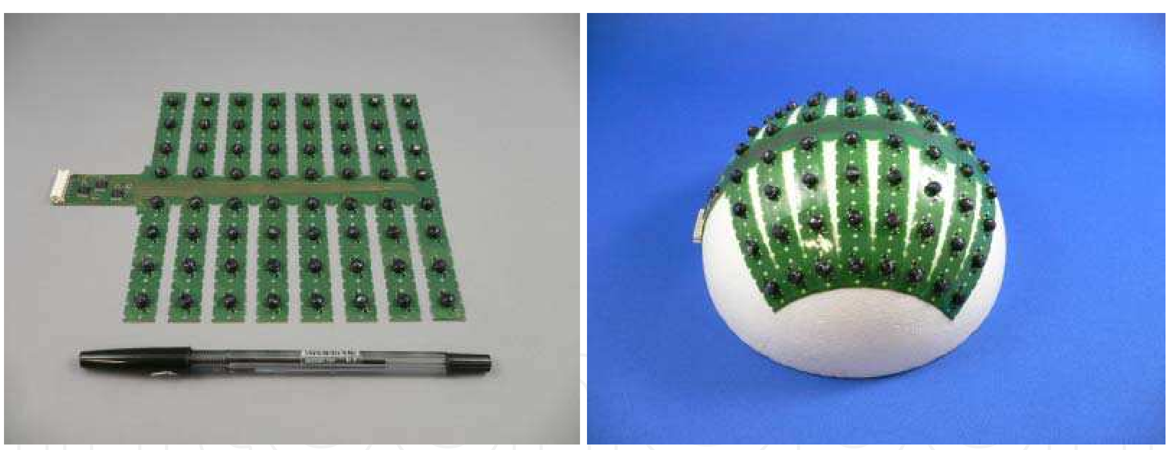

Fig. 4. Sensor sheet that can be cut into a comblike shape and wound on a curved surface

3.2 Method of fabricating a curved tactile sensor

To make the tactile sensors soft, we embedded the sensor sheet in an elastic body.

First, the sensor sheet is fixed after it is wound around the curved surface. Next, to remove gaps between the shells of pressure-sensing elements, the gaps are filled with a plastic material that hardens after the desired form is reached. Then, a small projection-shaped piece of elastic material is placed on the diaphragm of each pressure-sensing element. After that, an elastic sheet covers the above assembly. Fig. 5 shows a schematic of the structure of our curved tactile sensor. We used paper clay to fill the gaps, liquid rubber to fabricate the projection-shaped pieces, and a 5-mm-thick sponge sheet as the elastic sheet.

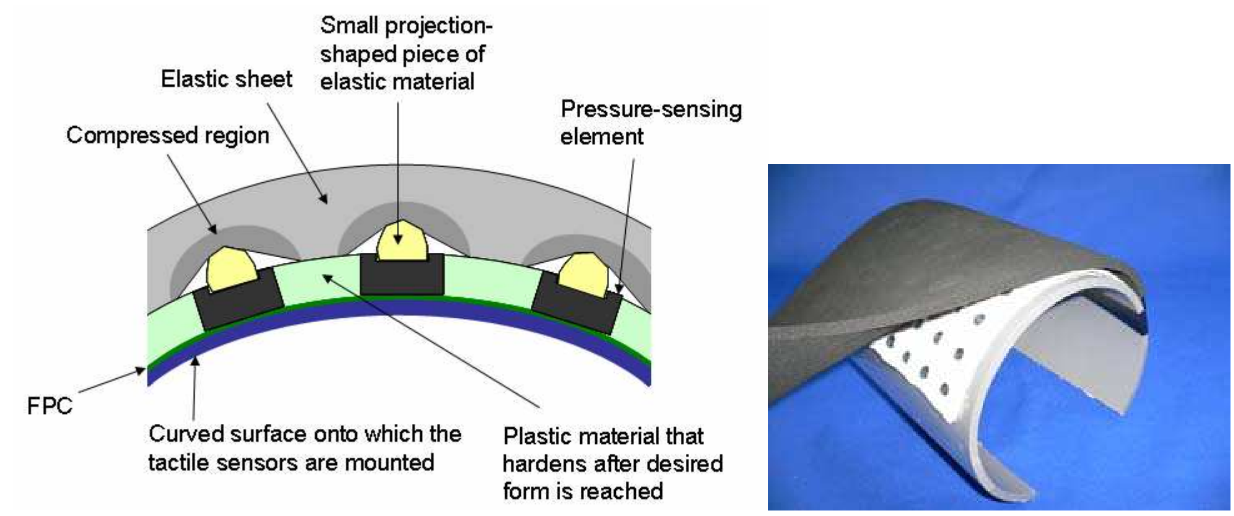

Fig. 5. Schematic structure and a photo of our curved tactile sensor

We selected the material of the elastic projection-shaped pieces to be harder than the elastic sheet. As a result, the small pieces push up against the elastic sheet, and the regions around the pieces in the sheet are compressed and become denser than the other regions. Thus, hard and soft areas appear in the elastic sheet (Fig. 5), and this structure has an amplifying effect (Mukai, 2005). A photograph of our curved tactile sensor is also shown in Fig. 5.

4. Implementation of a tactile sensor system

We installed the tactile sensors in our robot RI-MAN in five places, the chest and the right and left of the upper arms and forearms. Each sensor sheet has 8x8 elements, so that RI-MAN has 320 pressure-sensing elements in total. To process enormous sensor data in realtime in the vicinity of sensor, we developed a tactile sensor controller based on a dsPIC board (Landmark LM517), a picture of which is shown in Fig. 6.

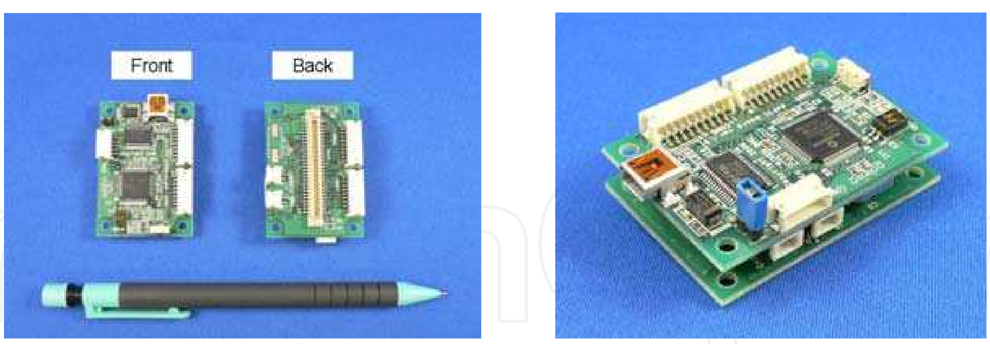

(a) Front and back view (b) Stacking with extension board

Fig. 6. dsPIC board for general sensing/controlling purposes

The dsPIC board is a general purpose sensing/controlling board developed by us, with a size of 35x50 mm^2. It is equipped with a dsPIC (Microchip technology 30F6012A) as the CPU and a USB interface IC (FTDI FT232RL) that realizes 1 Mbps communication. It also has many connectors through which many pins can be accessed. It also has a stacking connector for an extension board. The tactile sensor controller we developed uses a 12 bit A/D converter and digital I/Os in the 30F6012A. Its program is written in the C language and downloaded in the flash memory of the 30F6012A, as the firmware. The C program determines how to compress data from a tactile sensor sheet into abstract features suitable for network communication.

Using this board, up to 1 ms sampling of 1 tactile sensor sheet can be realized. We also developed an extension board for network communication, to connect the tactile sensors to the network in our robot RI-MAN. It has a network IC (Step Technica MKY40) that realizes a virtual shared memory, the maximum size of which is 512 byte. The guaranteed synchronization time of the virtual shared memory depends on the memory size, and is 1 ms for 256 byte and 2.4 ms for 512 byte. The extension board can be stacked with the dsPIC board as shown in Fig. 6(b). The small size and the network communication ability of our tactile sensor controller enable us to install them distributedly in the robot body. The communication can be realized using only 2 cables, which largely simplifies wiring and reduces maintenance cost in the robot.

In the virtual shared memory space, each node occupies an area consisting of stations one of which corresponds to 8 byte. In RI-MAN, various sensor controllers and motor controllers are connected to the network and, as a result, the area that tactile sensors can use is limited. In the current implementation, the host PC (with RT-Linux) occupies 1 station to send commands (for setting modes and parameters) through network to tactile sensors, and each of 5 tactile sensor controllers occupies 3 stations.

Each tactile sensor has only 3 stations, corresponding to 24 byte, for communication, thus all of 8x8 sensor element values (which is expressed by 12 bit) cannot be transmitted simultaneously. It is possible to send data line by line and combine them in the host PC to obtain whole output of one sensor sheet, but this takes unacceptable time (about 90ms) for feedback control. So we determined to calculate geometric moments in local controllers and transmit only the moments through network. The geometric moments are expressed, using element value I_{xy} at (x, y), as follows.

Zeroth: $M_0 = \sum_{x,y} I_{xy}$

First: $M_x = \sum_{x,y} x I_{xy}$, $M_y = \sum_{x,y} y I_{xy}$

Second: $M_{xy} = \sum_{x,y} xy I_{xy}$, $M_{x^2-y^2} = \sum_{x,y} (x^2 - y^2) I_{xy}$

The zeroth moment is the total sum itself, and the centroids (center of pressure) can be obtained by dividing the first by the zeroth. Using up to the second moments, we can obtain the axis of least inertia (Horn, 1986), which is the orientation of the object, as shown in Fig. 7. In the controller using dsPIC, all of data acquisition and calculation finishes in 2 ms.

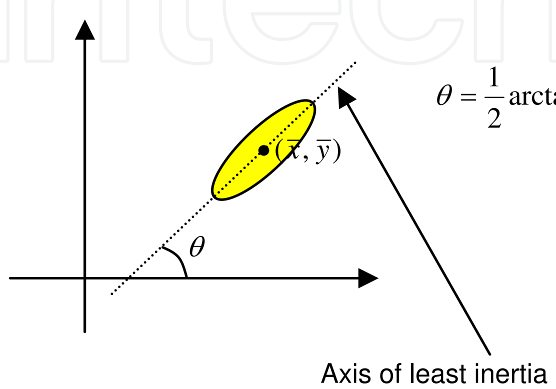

$$\theta = \frac{1}{2} \arctan(2(M_{xy} - M_0 \bar{x}\bar{y}), (M_{x^2-y^2} - M_0(\bar{x}^2 - \bar{y}^2))$$

Fig. 7. The axis of least inertia

5 Experimental results

5.1 Basic performance of the sensor

We conducted experiments to investigate the basic performance of our tactile sensor system. Flat tactile sensors with the 5-mm-thick elastic sheet were used to investigate the basic performance. In experiments where a dynamic force was needed, the experimental setup shown in Fig. 8 was used. The setup consisted of a digital force gauge, a load cell (Minebea LSM-1K-B), a vibrator (Asahi SeisakusyoWaveMaker01), and an XY stage. The force gauge was used to approximately measure the applied force to ensure that an excessive force was not exerted. Actual measurement of the applied force was carried out using the load cell, which has higher accuracy. The vibrator was used to generate controlled dynamic motion, and the force was exerted using a rod with a circular tip with a diameter of 8 mm. In experiments where a force over a wider area was needed, weights were used. However, in this case, the force was limited to a static force. Outputs from pressure-sensing elements were digitized by an A/D converter in the tactile sensor controller and sent to a PC through USB connection. These values are referred to as 'sensor output'. The unit of sensor output corresponds to 0.00122 V, and the sampling period of the measurement was 1 ms. The amplifier gain of sensor sheets were fixed to 8 in all experiments.

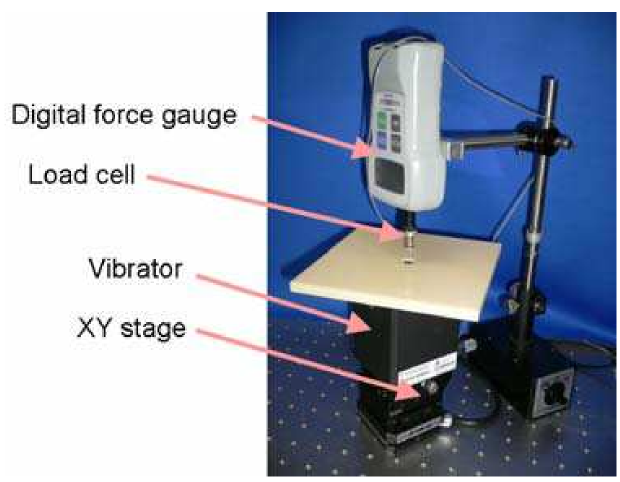

Fig. 8. Experimental setup

a) Response to a sinusoidal wave

First, we show, in Fig. 9, the measured time response of a pressure-sensing element (with the covering sheet) along with the applied force, when vibrated with a 1, 10, or 100 Hz sinusoidal wave. The force was applied from immediately above the element using the rod with the 8 mm circular tip. We can see that the time response has a smooth sinusoidal shape at 1 and 10 Hz, though the shape is slightly deformed at 100 Hz. A typical relationship between the applied force and the sensor output at 1 Hz is shown in Fig. 10. The sensor output is almost linear with the applied force. The solid line in the graph is the linear approximation $y = ax$ based on the results (from 3000 samples), where $a = 13.35$ in this case. This slope is referred to as gain in this paper. From this experiment, we can also see that our sensor has satisfactory measurable range and measurement resolution discussed in Section 2. When a force of 8 N was applied using the rod with the 8 mm circular tip, the pressure was about 159 kPa and the sensor output was more than 90. These results satisfy the required maximum range of 88 kPa and 5 bit resolution.

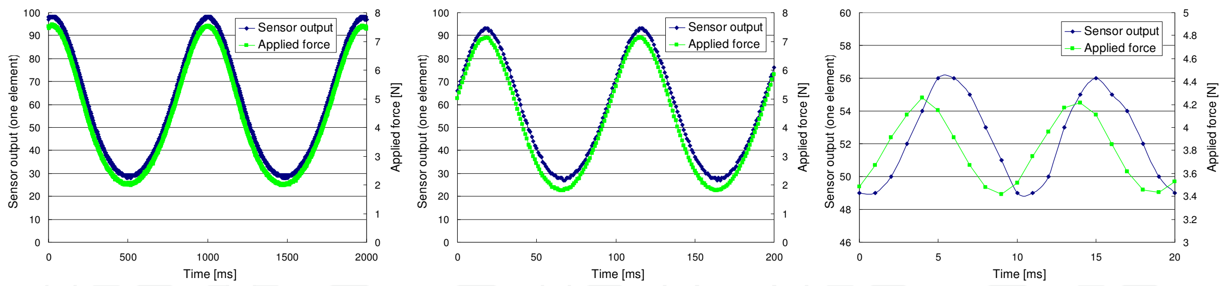

(a) 1 Hz (b) 10 Hz (c) 100 Hz

Fig. 9. Response of a pressure-sensing element to sinusoidal force

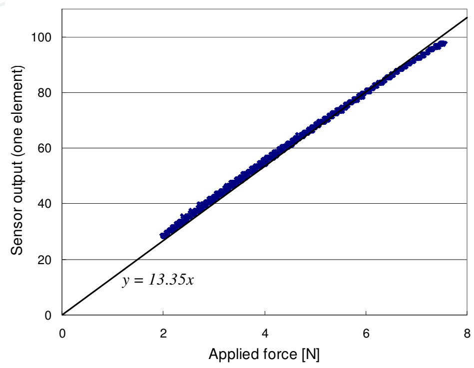

Fig. 10. Force vs sensor output

b) Variations of pressure-sensing elements

Next, we checked the variations of pressure-sensing elements on a sensor sheet. A sinusoidal force of 1 Hz was applied from immediately above the element using the rod with the 8 mm circular tip. The results of 20 elements are shown in Fig. 11. The standard deviation is about 6.5% of the averaged gain. The gains varied partly because we manually fabricated the projection-shaped elastic pieces on the diaphragms. We expect that if we make them by a more controlled method, the variation will decrease.

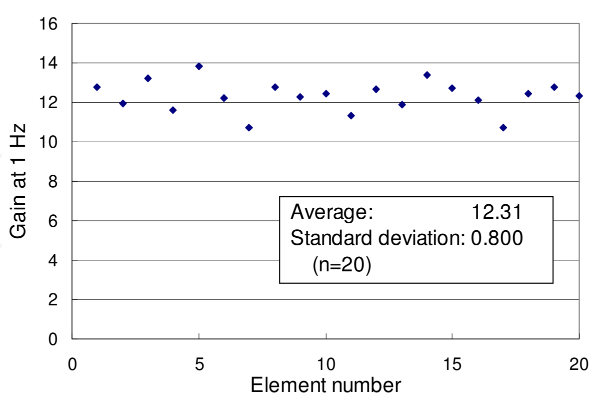

Fig. 11. Variations of elements on a sensor sheet

c) Frequency response

The results of experiments to investigate frequency response are shown in Fig. 12. The output was measured from a certain pressure-sensing element in a tactile sensor, and gain was normalized to 1 at 1 Hz. The decrease of gain at 100 Hz is 3 dB and the phase delay is 20 degree, approximately. These results show that our sensor can detect high-frequency signals.

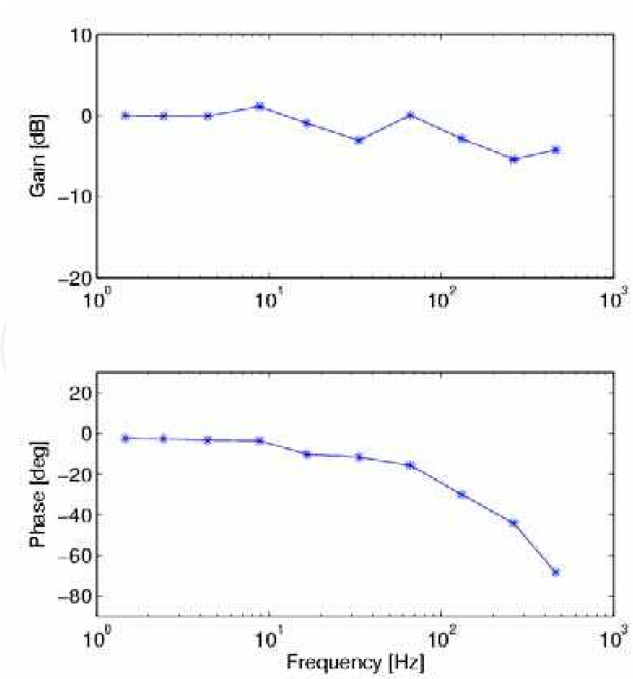

Fig. 12. Frequency response of a sensing element

d) Interpolation ability

Interpolation ability is obtained because of the covering elastic sheet even though discrete pressure-sensing elements are located separately. This removes undesirable insensitive region on the tactile sensor. Experimental results for verifying this effect are shown in Fig. 13. By applying a force using the rod with a tip diameter of 8 mm at a certain distance away from the element, gains in the graph were measured. The gain was normalized to 1 at the distance 0. The response shape agrees with the theoretically calculated values in (Shimojo, 1997).

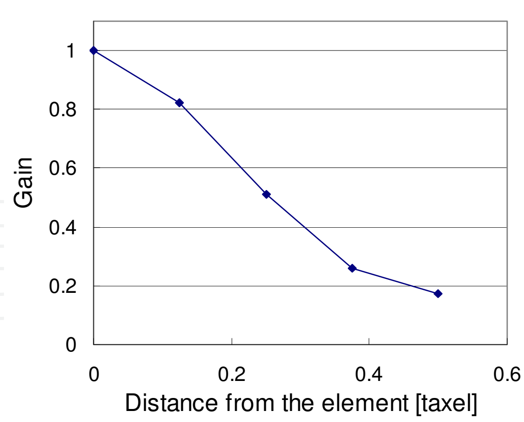

Fig. 13. Results of interpolation test

e) Hysteresis and drift

The results of experiments for investigating hysteresis are shown in Fig. 14. A load of 6.75 N approximately was applied and removed in about 5 s. Hysteresis exists but it is small. Next, to see longer-term effect (drift), a 668 g weight with an area of 52x44 mm^2 was placed on the sensor for 10 minutes. The sum of outputs from all elements is shown in Fig. 15. The output reduced slightly but it is about 4% of the initial output.

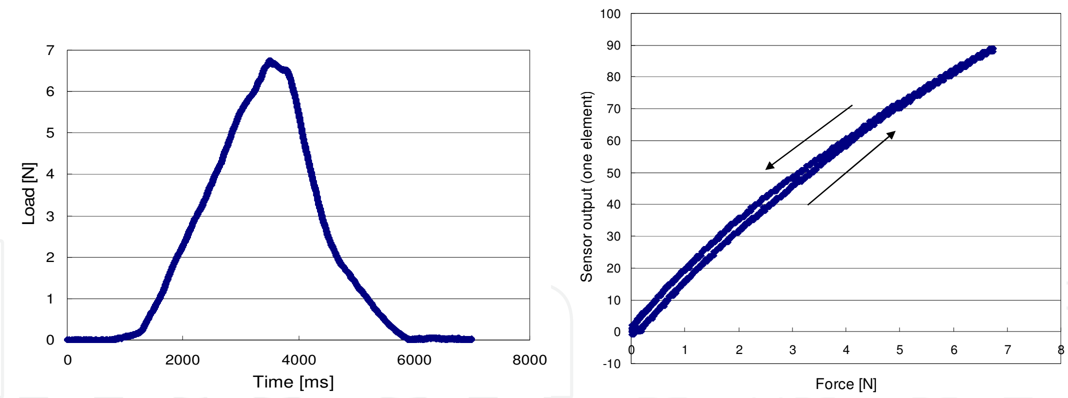

(a) Time profile of applied force (b) Force vs sensor output

Fig. 14. Results of hysteresis test

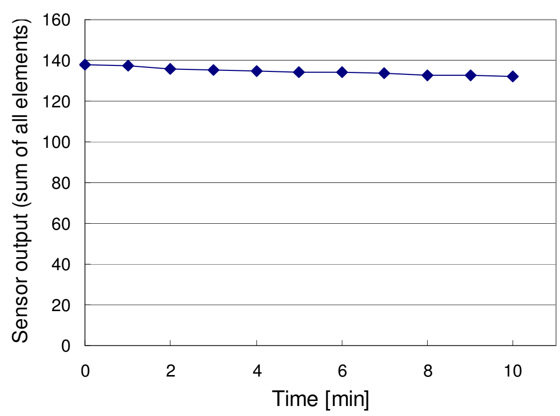

Fig. 15. Drift over 10 minutes

5.2 Tactile sensors in a robot

The output of all tactile sensors when holding a dummy human weighing 18 kg in its arms is shown in Fig. 16. The size of each square represents the amplitude of the corresponding tactile sensor element in log scale. This data were obtained and recorded in the host PC by

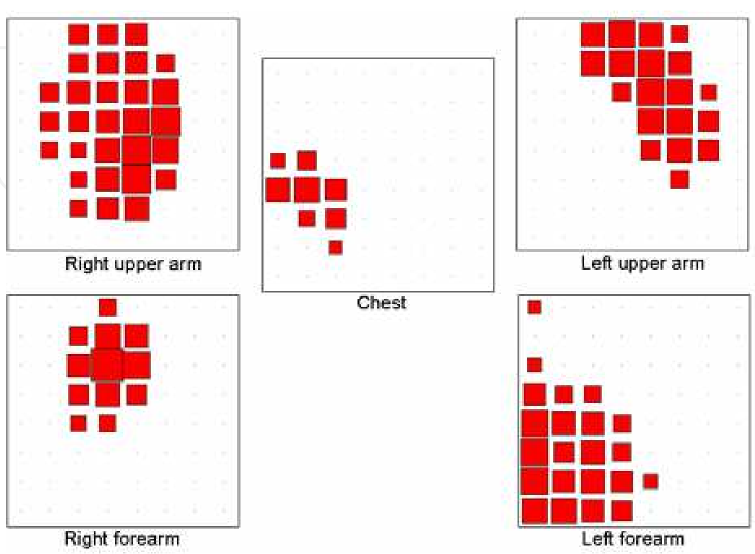

Fig. 16. Tactile sensor output when holding a dummy human weighing 18 kg

line-by-line transmission. The transmission took about 90 ms, but data acquisition itself in local tactile sensor controllers finished in 1 ms.

Next, we investigated the relationship between the roll angle and the sensor output when RI-MAN rotated its waist joint right and left 15 degrees while holding the 18 kg dummy human (Fig. 17). The results are in Fig. 18, where the realized roll angle and the pressure centroid on the left forearm are shown in graph (a), and the loads (the sum of all element outputs) detected by all tactile sensors in graph (b). In the sensor coordinates, the x-axis is along the left forearm from the base to the end, and the y-axis is from outside to inside. We can see that tactile sensors succeeded in detecting the changes of the object load and position caused by the roll angle change. The data show that the position of the dummy human shifted little by little during the cycles, even though the waist angle repeated the same motion.

+15 degrees 0 degrees -15 degrees

Fig. 17. Experiment scenes to obtain sensor output from a dummy human

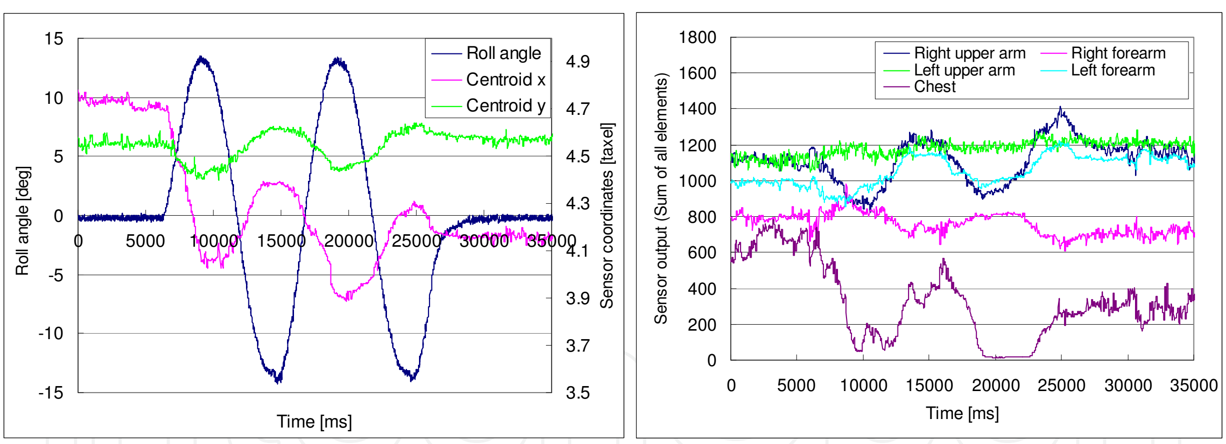

(a) Roll angle and the centroids on the left forearm

(b) Load on each tactile sensor

Fig. 18. Sensor output caused by a dummy human when waist angle is changed

7. Conclusion

In this paper, we described the successful development of the tactile sensor system of our human-interactive robot RI-MAN. The necessary specifications for RI-MAN tactile sensors are satisfied by our tactile sensor system. RI-MAN, equipped with the tactile sensors, succeeded in detecting the magnitude and position of the load when it was holding a dummy human.

For future work, we will develop control methods for manipulating objects with arms using tactile sensor feedback. We will also develop sensor signal processing methods for detecting not only physical contact but also human tactile sensations such as hitting and stroking. This enables the tactile sensor to be used in human-robot communication, as well as in physical labors.

7. References

Horn B. K. P. (1986). *Robot Vision,* MIT Press, Cambridge, MA

Inaba, M.; Hoshino, Y.; Nagasaka, K.; Ninomiya, T.; Kagami, S. & Inoue, H. (1996). A full-body tactile sensor suit using electrically conductive fabric and strings, in *Proc. IEEE/RSJ International Conference on Intelligent Robots and Systems,* pp. 450–457

Kanda, T.; Ishiguro, H.; Ono, T.; Imai, M. & Nakatsu, R. (2002). Development and evaluation of an interactive humanoid robot 'Robovie', in *Proc. IEEE International Conference on Robotics and Automation,* pp. 4166–4173

Lumelsky, V. J.; Shur, M. S. & Wagner, S. (2001). Sensitive skin, *IEEE Sensors Journal,* Vol. 1, No. 1, pp. 41–51

Mitsunaga, N.; Miyashita, T.; Ishiguro, H.; Kogure, K. & Hagita, N. (2006). Robovie-IV: A communication robot interacting with people daily in an office, in *Proc. IEEE/RSJ International Conference on Intelligent Robots and Systems,* pp. 5066–5072

Mukai, T. (2004). Soft areal tactile sensors with embedded semiconductor pressure sensors in a structured elastic body, in *Proc. IEEE International Conference on Sensors,* pp. 1518–1521

Mukai, T. (2005). Development of soft areal tactile sensor on curved surfaces, in *Proc. IEEE International Conference on Robotics and Biomimetics,* pp. 14-18

Mukai, T.; Onishi, M.; Odashima, T.; Hirano, S. & Luo, Z. (2008). Development of the Tactile Sensor System of a Human-Interactive Robot "RIMAN", *IEEE Trans. on Robotics,* Vol. 24, No. 2, pp.505-512

Nakamura, K. & Shinoda, H. (2001). A tactile sensor instantaneously evaluating friction coefficients, in *Proc. International Conference on Solid-State Sensors and Actuators,* Vol. 2, pp. 1430–1433

Odashima, T.; Onishi, M.; Tahara, K.; Takagi, K.; Asano, F.; Kato, Y.; Nakashima, H.; Kobayashi, Y.; Luo, Z. W.; Mukai, T. & Hosoe, S. (2006). A soft human-interactive robot – RI-MAN –, in *Video Proc. IEEE/RSJ International Conference on Intelligent Robots and Systems*

Odashima, T.; Onishi, M.; Tahara, K.; Mukai, T.; Hirano, S.; Luo, Z. & Hosoe, S. (2007). Development and evaluation of a human-interactive robot platform 'RI-MAN', *Journal of the Robotics Society of Japan,* Vol. 25, No. 4, pp. 554−565 (in Japanese)

Ohmura, Y.; Kuniyoshi, Y. & Nagakubo, A. (2006). Conformable and scalable tactile sensor skin for curved surfaces, in *Proc. IEEE International Conference on Robotics and Automation,* pp. 1348–1353

Ohmura, Y. & Kuniyoshi, Y (2007). Humanoid robot which can lift a 30kg box by whole body contact and tactile feedback, in *Proc. IEEE/RSJ International Conference on Intelligent Robots and Systems,* pp. 1136-1141

Paul, R. P. (1981). *Robot manipulators: Mathematics, programming, and control,* MIT Press, Cambridge, MA

Reimer, E. M. & Danisch, L. (1999). Pressure sensor based on illumination of a deformable integrating cavity, U.S. Patent 5917180

RSJ (the Robotics Society of Japan) ed. (2005). *Robotics handbook - 2nd ed.,* CORONA Publishing, Tokyo, pp.652–654 (in Japanese)

Shimojo, M. (1997). Mechanical filtering effect of elastic cover for tactile sensor, *IEEE Trans. Robotics and Automation,* Vol. 13, No. 1, pp. 128–132

Shimojo, M.; Namiki, A.; Ishikawa, M.; Makino, R. & Mabuchi, K. (2004). A tactile sensor sheet using pressure conductive rubber with electrical-wires stitched method, *IEEE Sensor Journal,* Vol. 4, No. 5, pp. 589-596

Souza, R. J. D. & Wise, K. D. (1997). A very high density bulk micromachined capacitive tactile imager, in *Proc. of International Conference on Solid-State Sensors and Actuators,* pp. 1473–1476

Suzuki, K. (1993). High-density tactile sensor arrays, *Advanced Robotics,* Vol. 7, No. 3, pp. 283–287

Tajima, R.; Kagami, S.; Inaba, M. & Inoue, H. (2002). Development of soft and distributed tactile sensors and the application to a humanoid robot, *Advanced Robotics,* Vol. 16, No. 4, pp. 381–397

Tekscan (2008). http://www.tekscan.com/medical/systems.html

Yamada, D.; Maeno, T. & Yamada, Y. (2002). Artificial finger skin having ridges and distributed tactile sensors used for grasp force control, *Journal of Robotics and Mechatronics,* Vol. 14, No. 2, pp. 140–146

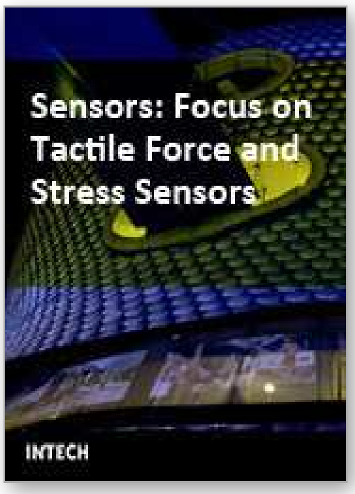

Sensors: Focus on Tactile Force and Stress Sensors

Edited by Jose Gerardo Rocha and Senentxu Lanceros-Mendez

ISBN 978-953-7619-31-2

Hard cover, 444 pages

Publisher InTech

Published online 01, December, 2008

Published in print edition December, 2008

This book describes some devices that are commonly identified as tactile or force sensors. This is achieved with different degrees of detail, in a unique and actual resource, through the description of different approaches to this type of sensors. Understanding the design and the working principles of the sensors described here requires a multidisciplinary background of electrical engineering, mechanical engineering, physics, biology, etc. An attempt has been made to place side by side the most pertinent information in order to reach a more productive reading not only for professionals dedicated to the design of tactile sensors, but also for all other sensor users, as for example, in the field of robotics. The latest technologies presented in this book are more focused on information readout and processing: as new materials, micro and sub-micro sensors are available, wireless transmission and processing of the sensorial information, as well as some innovative methodologies for obtaining and interpreting tactile information are also strongly evolving.